Rice P$_{1B}$-Type Heavy-Metal ATPase, OsHMA9, Is a Metal Efflux Protein[1][W][OA]

Sichul Lee, Yu-Young Kim, Youngsook Lee, and Gynheung An*

Division of Molecular and Life Science, Biotechnology Research Center, Pohang University of Science and Technology, Pohang 790–784, Korea

P$_{1B}$-type heavy-metal ATPases (HMAs) are transmembrane metal-transporting proteins that play a key role in metal homeostasis. Despite their importance, very little is known about their functions in monocot species. We report the characterization of rice (*Oryza sativa*) OsHMA9, a member of the P$_{1B}$-type ATPase family. Semiquantitative reverse transcription-polymerase chain reaction analyses of seedlings showed that *OsHMA9* expression was induced by a high concentration of copper (Cu), zinc (Zn), and cadmium. We also determined, through promoter::β-glucuronidase analysis, that the main expression was in the vascular bundles and anthers. The OsHMA9:green fluorescence protein fusion was localized to the plasma membrane. Heterologous expression of *OsHMA9* partially rescued the Cu sensitivity of the *Escherichia coli copA* mutant, which is defective in Cu-transporting ATPases. It did not rescue the Zn sensitivity of the *zntA* mutant, which is defective in Zn-transporting ATPase. To further elucidate the functional roles of *OsHMA9*, we isolated two independent null alleles, *oshma9-1* and *oshma9-2*, from the T-DNA insertion population. Mutant plants exhibited the phenotype of increased sensitivity to elevated levels of Cu, Zn, and lead. These results support a role for OsHMA9 in Cu, Zn, and lead efflux from the cells. This article is the first report on the functional characterization of a P$_{1B}$-type metal efflux transporter in monocots.

A number of heavy metals, including copper (Cu), zinc (Zn), manganese, and iron, are essential micronutrients for a wide variety of physical processes. These micronutrients can serve structural roles in proteins, act as enzyme cofactors, and function in cellular redox reactions (Williams and Mills, 2005). However, when present in excess, they can have deleterious effects because of their reactive nature (Schutzendubel and Polle, 2002). For example, Cu is an essential element for plant growth and is important in various biochemical reactions but, at toxic levels, it interferes with numerous physiological processes (Fernandes and Henriques, 1991). Likewise, Zn acts as a nutrient, but can be very toxic at higher concentrations (Rout and Das, 2003). Furthermore, some metals, such as cadmium (Cd), mercury, silver, and lead (Pb), are generally considered nonessential to plants and are potentially highly toxic because of their reactivity with sulfur and nitrogen in amino acid side chains (Clemens, 2001).

Accumulations of these heavy metals in plants can occur following their uptake from contaminated soil, which can then lead to toxic levels in animals feeding on them (Mills et al., 2005). To maintain the concentration of essential metals within physiological limits and to minimize the detrimental effects of nonessential metals, plants, like other organisms, trigger a complex network of homeostatic mechanisms to control their uptake, accumulation, trafficking, and detoxification (Clemens, 2001). Specialized transport proteins, in the form of channels, carriers, or pumps, mediate the movement of heavy metals through membranes (Williams et al., 2000). Several types of heavy-metal transporters have now been cloned from plants (Williams et al., 2000; Clemens, 2001).

The ion pumps in the P-type ATPase superfamily share a common enzymatic mechanism in which ATP hydrolysis aids in transporting ions across the membrane (Pedersen and Carafoli, 1987). P-type ATPases, found in all types of living organisms, are used to translocate a diverse set of ions, including H$^+$, Na$^+$/K$^+$, H$^+$/K$^+$, and Ca^{2+}, plus heavy metals and possibly lipids (Axelsen and Palmgren, 1998; Kuhlbrandt, 2004). This superfamily is divided into five major branches and 10 subfamilies, according to the substrate being transported. All the heavy-metal pumps from bacteria, plants, and humans share significant sequence similarities and are clustered together as the P$_{1B}$ subfamily (Axelsen and Palmgren, 1998). P$_{1B}$-type heavy-metal ATPases (HMAs) have been implicated in the transport of a range of essential as well as potentially toxic metals across cell membranes. This HMA group can be subdivided into two distinct clusters through phylogenetic analyses (Rensing et al., 1999). The Cu cluster has members with

---

a role in Cu and silver transport, whereas the Zn cluster proteins transport Zn and other heavy metals (e.g. cobalt, Cd, and Pb; Axelsen and Palmgren, 2001).

Of the eight P_{1B}-ATPases in Arabidopsis (*Arabidopsis thaliana*), four belong to the Cu cluster and four to the Zn cluster (Baxter et al., 2003). AtHMA6/PAA1, the first HMA cloned from Arabidopsis (Tabata et al., 1997), plays a critical role in the Cu transport system in chloroplasts, being responsible for cofactor delivery to stomatal Cu/Zn superoxide dismutase (Shikanai et al., 2003). AtHMA8/PAA2, closely related to AtHAM6, transports Cu into the thylakoid lumen to supply plastocyanin (Abdel-Ghany et al., 2005). *AtHMA5* is strongly and specifically induced by Cu in whole plants and T-DNA insertion alleles of *AtHMA5* are hypersensitive to Cu, suggesting that AtHMA5 plays a key role in transmembrane transport while also interacting with plant metallochaperones (Andres-Colas et al., 2006). AtHMA7/RAN1 may be important in the delivery of Cu ions to ethylene receptors (Hirayama et al., 1999). Complementation of the yeast (*Saccharomyces cerevisiae*) *ccc2* mutant by AtHMA7 confirms its function as a Cu transporter. Although AtHMA1 phylogenetically falls in the Zn cluster, yeast expression experiments demonstrated that AtHMA1 is involved in Cu homeostasis (Seigneurin-Berny et al., 2006). Proteomic analyses of the Arabidopsis chloroplast envelope identified AtHMA1 as one of the candidates for metal transporters. Characterization of Arabidopsis *hma1* mutants revealed lower Cu content in chloroplasts and diminution of the total chloroplast superoxide dismutase activity. ATPase activity of AtHMA1 in purified chloroplast envelope membranes was specifically stimulated by Cu, demonstrating that the protein is an envelope ATPase, delivering Cu ions to the stroma (Seigneurin-Berny et al., 2006).

The Zn cluster P_{1B}-ATPases play a role in metal detoxification. The increase in Zn^{2+} and Cd^{2+} levels in *hma2* plants indicates that AtHMA2 drives the efflux of Zn^{2+} from the plant cells and also controls the levels of nonphysiological heavy metals, such as Cd^{2+} (Eren and Arguello, 2004). Disruption of AtHMA4 function resulted in increased sensitivity to elevated levels of Cd and Zn (Verret et al., 2004; Mills et al., 2005). An *hma2 hma4* double mutant showed a chlorotic, stunted phenotype that can be rescued by exogenous Zn application, indicating that the primary role of these transporters is likely to be in the translocation of Zn (Hussain et al., 2004). AtHMA3 functions as a Cd/Pb transporter in yeast, whereas the AtHMA3::GFP is localized to the vacuole, suggesting a role in the influx of Cd into the vacuolar compartment (Gravot et al., 2004). Unfortunately, most of the knowledge concerning plant P_{1B}-type ATPases has been acquired from dicot species (Colangelo and Guerinot, 2006; Grotz and Guerinot, 2006; Broadley et al., 2007; Krämer et al., 2007). Therefore, the functional characterization of P_{1B}-type HMA from monocot species is important to determine whether those same crucial roles are found in dicot species.

Rice (*Oryza sativa*) is an important food source for half the world's population. It is the first crop species to be sequenced and, therefore, has great impact in agricultural research (Goff et al., 2002; Yu et al., 2002; International Rice Genome Sequencing Project, 2005). Analysis of its genome sequences have resulted in the identification of nine P_{1B}-type HMA genes (Williams and Mills, 2005). By contrast, 10 members of P_{1B}-type HMAs have been reported in barley (*Hordeum vulgare*; Williams and Mills, 2005). In this study, we characterized a rice P_{1B}-type ATPase, *OsHMA9*, through molecular and genetic approaches. We have previously reported the establishment of T-DNA insertional mutant lines in japonica rice (Jeon et al., 2000; Jeong et al., 2002; Ryu et al., 2004). To facilitate the use of those lines, we have also determined the sites where T-DNA is inserted and have established a database of the insertion sites (An et al., 2003; Jeong et al., 2006). From that mutant population, we have now obtained two independent T-DNA insertions in the *OsHMA9* gene. Using knockout plants, we have investigated here the role of *OsHMA9* for heavy-metal transport in rice.

RESULTS

Expression Analysis of Rice P_{1B}-Type ATPase Genes

A database search for rice protein sequences belonging to the P_{1B}-type ATPases identified a family of nine proteins (Baxter et al., 2003; Williams and Mills, 2005). Phylogenetic analysis showed that OsHMA1 through OsHMA3 belong to the Zn cluster, whereas OsHMA4 through OsHMA9 are part of the Cu cluster. Several of their ESTs were present in cDNA libraries prepared from panicles, seedling roots, or green shoots, indicating that these genes are functional in various organs. We investigated the expression patterns of the Cu subgroup (*OsHMA4–OsHMA9*) using semiquantitative reverse transcription (RT)-PCR with gene-specific primers located at the 3' end of each gene, which does not cover any conserved sequences (Fig. 1). Because introns occurred between the primers, genomic DNA contamination could be distinguishable from the cDNA (i.e. PCR bands longer than the expected cDNA size were likely from the genomic DNA). We used short PCR cycles to avoid saturation and the products were hybridized with each *OsHMA* probe.

During vegetative growth, *OsHMA4*, *OsHMA5*, and *OsHMA9* were more strongly expressed in the roots of 30-d-old seedlings than in the leaves, whereas *OsHMA6*, *OsHMA7*, and *OsHMA8* were more strongly expressed in the leaves (Fig. 1A). The *OsHMA9* mRNA level was higher in fully expanded mature leaves at the flowering stage compared with young leaves, suggesting that expression is increased as leaves senesce (Fig. 1A). To further investigate this possibility, we examined 60-d-old plants producing six leaves from the main shoot. Our analysis showed that the
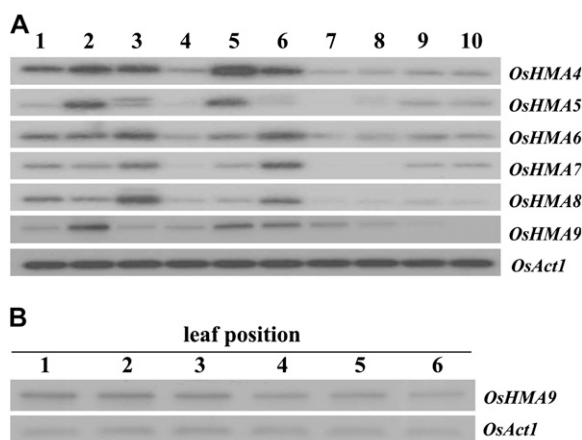
Figure 1. Expression analysis of *OsHMA4-9*. A, Spatial expression patterns of genes *OsHMA4* through *OsHMA9*. Semiquantitative RT-PCR was performed with cDNA prepared from various vegetative and reproductive organs: 1 and 2, Shoots and roots of 7-d-old seedlings; 3, 4, and 5, leaves, stems, and roots of 30-d-old plants; 6, fully expanded mature leaves at flowering stage; 7 and 8, panicles about 5 and 15 cm long; 9 and 10, immature seeds 3 and 9 d after pollination. *OsAct1* is shown as internal control. B, Expression of *OsHMA9* according to leaf position in 60-d-old plants. Positions are indicated by order of appearance. Experiments were performed at least twice or more when results were not consistent. The most representative results are shown.

OsHMA9 transcript level was higher in older leaves, implying that OsHMA9 might function in metal mobilization as those tissues mature. In Arabidopsis, *AtHMA7/RAN1* also is induced during leaf senescence, contributing to nutrient mobilization (Himelblau and Amasino, 2001). All of the genes were weakly expressed in the stems and were also more weakly expressed in the reproductive organs than in the vegetative tissues (Fig. 1A). Expression of *OsHMA4*, *OsHMA6*, and *OsHMA8* were relatively constant throughout the various stages of panicle and seed development. However, expression levels of *OsHMA5* and *OsHMA7* were stronger in the seeds, whereas that of *OsHMA9* decreased in older panicles and seeds.

To evaluate the relationships between *OsHMA* genes and heavy metals, we performed dose-response experiments. Seven-day-old seedlings grown on Murashige and Skoog medium (containing 0.1 μM Cu and 30 μM Zn) were transferred to liquid medium supplemented with different concentrations of Cu, Zn, Pb, or Cd. Samples were harvested 3 or 6 h after this treatment (Fig. 2). Afterward, expression of *OsHMA4*, *OsHMA7*, and *OsHMA8* was only slightly, but not significantly, enhanced under these conditions. In contrast, expression of *OsHMA5* and *OsHMA6* was induced by such treatment. Finally, in the case of *OsHMA9*, high concentrations of Cu, Zn, or Cd increased transcript levels, but Pb had no effect. Therefore, we might suggest that at least three OsHMAs (OsHMA5, OsHMA6, and OsHMA9) play roles in heavy-metal detoxification. Among those three, we selected *OsHMA9* for further analysis.

## Expression Analysis of *OsHMA9* Using the *GUS* Reporter Gene

To study the spatial and temporal expression patterns of *OsHMA9* in planta, we fused the 0.9-kb fragment carrying the *OsHMA9* promoter to the *GUS* gene. Transgenic rice plants expressing that construct were generated by *Agrobacterium*-mediated cocultivation. Of the eight independent transformants examined here, seven manifested a consistent staining pattern. Histochemical GUS staining of 7-d-old seedlings showed that overall staining was much stronger after treatment for 6 h with 500 μM Cu (Fig. 3A), which coincided with RT-PCR results that demonstrated that the *OsHMA9* gene was inducible by a high Cu level. When seedlings were treated for 6 h with 10 mM Zn or 500 μM Cd, GUS activity was increased, compared with the untreated plants (Supplemental Fig. S1). In cross sections of the seminal roots, strong GUS activity was observed in the vascular cylinder (Fig. 3B). In the differentiation zone, where lateral roots develop, expression expanded to the cortex region, but was not detectable in young lateral roots (Fig. 3C). In the leaves and sheaths, GUS activity was as strongly detected in the vascular bundles as in the roots and was also detected in the mesophyll cells, but only weakly in the epidermal cells (Fig. 3, D–F).

In the developing spikelets, GUS activity was detectable mainly in the anthers (Fig. 3G). Cross sections at the young microspore stage showed activity in both the anther wall and the microspore (Fig. 3, H and I). At later stages, activity was mainly detectable in the anther wall (Fig. 3, J and K). In cross sections of the subordinate portions, GUS activity was present at low levels in the ovary (Fig. 3L). These results are, again, consistent with those from our RT-PCR analysis, demonstrating that *OsHMA9* is strongly expressed in the stamens (Supplemental Fig. S2).

OsHMA9 Is a Membrane Protein

For further insight into the functioning of OsHMA9, we analyzed its subcellular distribution by expressing a fusion protein with GFP. The program ARAMEMNON (http://aramemnon.botanik.uni-koeln.de) predicted with high probability that OsHMA9 may be localized to the plasma membrane. To confirm this, DNA constructs encoding OsHMA9:GFP and AtAHA2:red fluorescent protein (RFP) under the control of the cauliflower mosaic virus 35S promoter were simultaneously introduced into onion (*Allium cepa*) epidermal cells by particle bombardment. AtAHA2 is an Arabidopsis H$^+$-ATPase that localizes to the plasma membrane (Kim et al., 2001). After 16 h of incubation, expression of the introduced genes was examined under a fluorescent microscope with two different filters to visualize the GFP and RFP images (Fig. 4). The green fluorescent signal was detected from the plasma membrane (Fig. 4A) and coincided with an RFP signal driven by the AtAHA2 image (Fig. 4, B and

Figure 2. Dose-response analyses for expression of *OsHMA4-9*. Seven-day-old plants were treated for 3 or 6 h in liquid medium containing different concentrations of Cu, Zn, Pb, or Cd. Representative results from at least two replicates are shown for each section. In each experiment, three plants were used for RNA extraction of each indicated metal concentration and time.
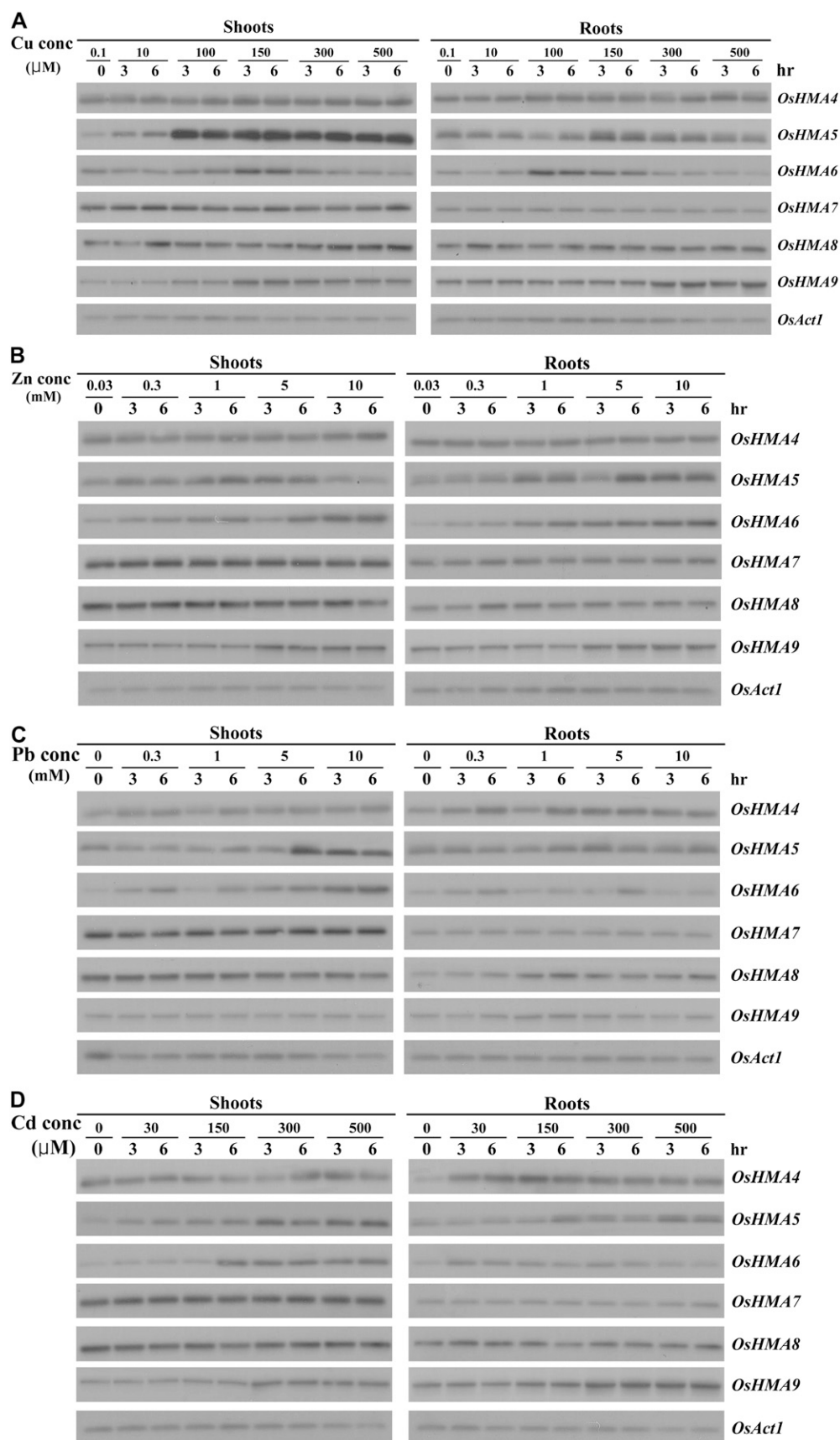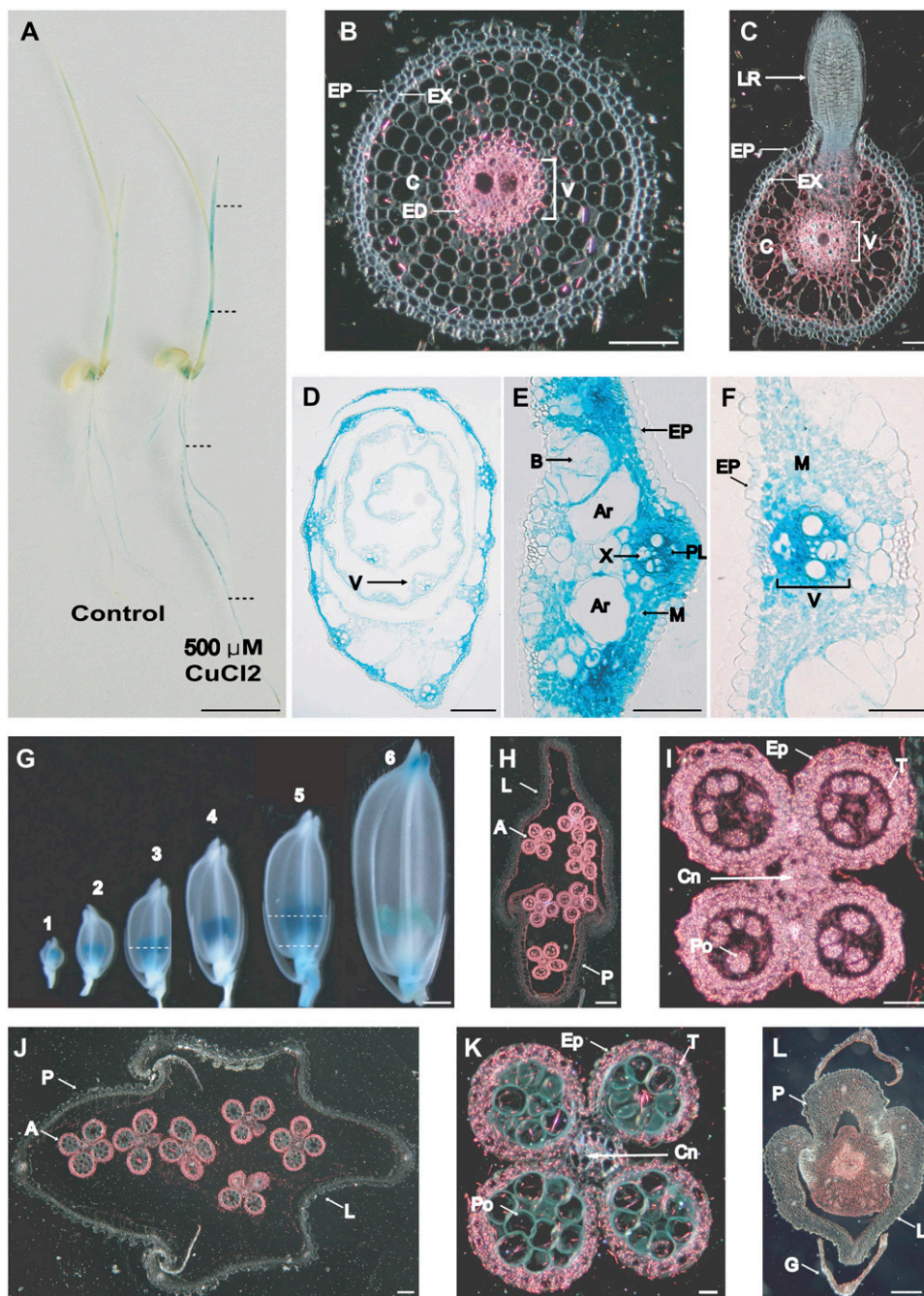
Figure 3. *OsHMA9* promoter-driven GUS expression pattern. A, Seven-day-old seedling grown in one-half-strength Murashige and Skoog medium (control; left) or treated with 500 μM CuCl$_2$ for 6 h (right). B to F, Cross sections of 10-d-old seedlings at indicated position (dotted line) in A; seminal root (B), lateral root (C), shoot (D), midrib region (E), and leaf blade (F). G, Temporal and spatial expression patterns of *OsHMA9-GUS* fusion construct in spikelets at various stages, as defined by extent of anther development. Sample 1, Meiosis; 2, tetrad; 3, early young microspore; 4, late young microspore; 5, vacuolated pollen; and 6, late pollen mitosis. H, Cross section of sample 3 from G at indicated position. I, Close-up image of anther from H. J, Cross section of sample 5 from G at indicated position. K, Close-up image of anther from J. L, Cross section of sample 5 from G at indicated position. B, C, and H to L, Dark-field images where GUS activities are visualized as red signals. In other images, GUS staining is shown in blue. A, Anther; Ar, aerenchyma; B, bulliform cell; C, cortex; Cn, connective tissues; ED, endodermis; EP, epidermis; EX, exodermis; G, glume; L, lemma; LR, lateral root; M mesophyll; P, palea; PL, phloem; Po, pollen; T, tapetum; V, vascular bundle; X, xylem. Bars = 1 cm in A; 50 μm in B to F and L; 1 mm in G; 100 μm in H and J; and 25 μm in I and K.

C). In contrast, fluorescence of GFP alone was observed throughout the cytoplasm and nucleus (Fig. 4D). These results, together with its demonstrated inducibility by metals, suggest that OsHMA9 is a metal transporter located in the plasma membrane.

Heterologous Expression of *OsHMA9* in *Escherichia coli*

Because the OsHMA9 protein belongs to the Cu ATPase subclass phylogenetically, we investigated whether OsHMA9 could transport Cu in *Escherichia coli*. *OsHMA9* cDNA was expressed in an *E. coli*

mutant with a disruption in *CopA*, which encodes the Cu efflux P$_{1B}$-type ATPase (Rensing et al., 2000). Expression of OsHMA9 partially rescued Cu sensitivity in the mutant (Fig. 5A), indicating that the protein is a Cu efflux transporter. Similar experiments using a range of Zn and Cd concentrations were also performed, but no differences in growth were seen between the *copA* mutant and the control, wild-type strains (data not shown). We also tested the growth rate of the *copA* mutant expressing *OsHMA9* in Luria-Bertani medium containing 2 mM CuSO$_4$ (Fig. 5B). Under such conditions, that rice gene was able to
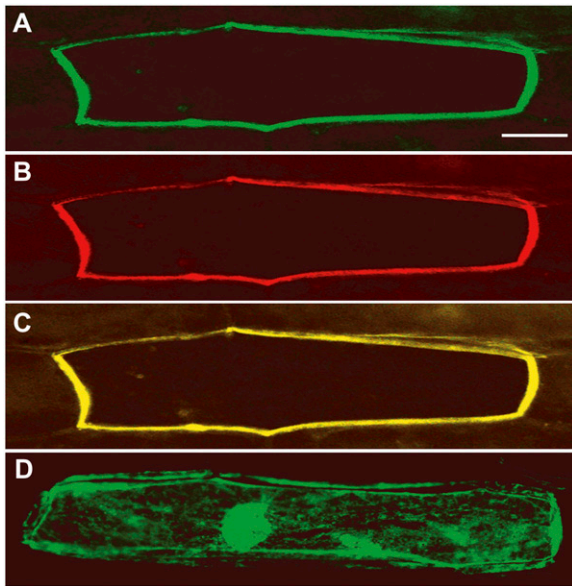
Figure 4. Subcellular localization of OsHMA9:GFP fusion protein. Onion cells were cotransformed with *OsHMA9:GFP* and *AHA2:RFP* fusion constructs via particle bombardment; fluorescent signals were examined 16 h after transfection. A, Green fluorescence image. B, Red fluorescence image. C, Merged images of A and B. As a control, expression of GFP alone was analyzed (D). Bars = 25 μm.

restore the mutant growth rate, suggesting a role in prompting Cu efflux from the cytoplasm.

Because *OsHMA9* is also induced by high Zn exposure, we examined whether OsHMA9 could transport Zn in *E. coli*. *OsHMA9* cDNA was expressed in an *E. coli* mutant with a disruption in *ZntA*, which encodes the Zn efflux P_{1B}-type ATPase (Rensing et al., 1997). Here, expression of OsHMA9 did not result in a significant increase in Zn resistance in the *zntA* mutant (Supplemental Fig. S3).

**Isolation of T-DNA Insertion Mutant Alleles of *OsHMA9***

To further examine the functional roles of *OsHMA9* in plants, we identified two independent T-DNA insertion alleles from the rice-flanking sequence tag database (An et al., 2003; Jeong et al., 2006). T-DNA was inserted into the first intron of *OsHMA9* in *oshma9-1* and into the ninth intron in *oshma9-2* (Fig. 6A). T2 progeny were obtained and homozygous knockout plants were selected by PCR, using gene-specific primers, located on the 3′ end of *OsHMA9*, as well as T-DNA primers (Fig. 6A). When its transcript levels were examined in T-DNA homozygous plants, both alleles were found to be null (Fig. 6B). Because the T-DNA was inserted at the end of *OsHMA9* in *oshma9-2*, we tested the presence of a truncated transcript using primers located before that T-DNA insertion (Supplemental Fig. S4). In fact, a truncated transcript was detected in *oshma9-2* but not in *oshma9-1*. Although a truncated protein may have been produced in the

former, it was unlikely to be functional because the phenotypes of *oshma9-2* and *oshma9-1* are identical. Therefore, we can conclude that, although the C-terminal region is not well conserved among the proteins in that family, it is necessary for protein functioning.

OsHMA9 Knockout Plants Are Sensitive to Elevated Levels of Cu, Zn, Pb, and Cd

Because the expression of *OsHMA9* was induced by heavy metals and its heterologous expression was restored in the *E. coli copA* mutant, we hypothesized that OsHMA9 might play a role in heavy-metal detoxification. The *oshma9/oshma9* homozygous plants and their segregating wild-type siblings were indistinguishable when grown in soil or on solid medium containing one-half-strength Murashige and Skoog salts.

To test the effect of heavy metals on the growth of rice seedlings, we performed a dose-response experiment. Wild-type and knockout plants were grown for 12 d in solid medium supplemented with different concentrations of Cu, Zn, Pb, or Cd to determine at what levels the aberrant phenotypes would become apparent. Plant height, fresh weight, and chlorophyll
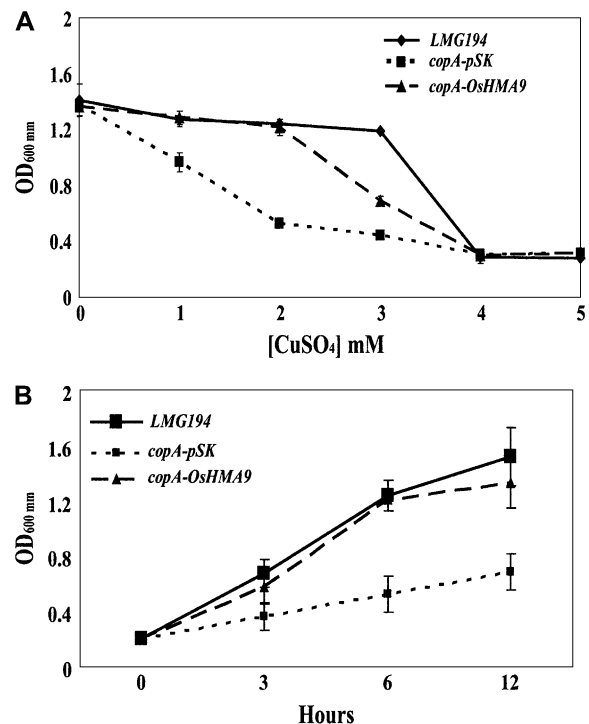
Figure 5. Heterologous expression of *OsHMA9* in *E. coli*. A, Growth of wild-type (LMG194), *copA* mutant transformed with vector alone (*copA*-pSK) and *copA* mutant transformed with pBluescript/*OsHMA9* (*copA*-*OsHMA9*) in Luria-Bertani medium with indicated concentration of $CuSO_4$. B, Growth of wild-type, *copA*-pSK, and *copA*-*OsHMA9* in Luria-Bertani medium supplemented with 2 mM $CuSO_4$. Representative results from two replicates are shown for each image. Four samples were used in each replicate.
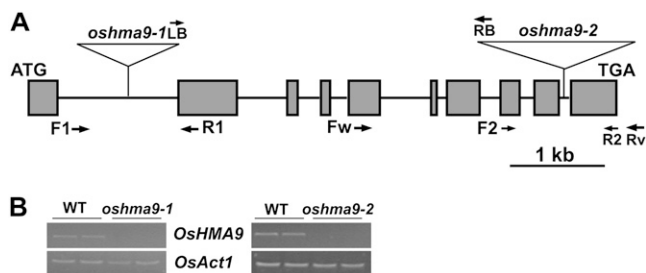
Figure 6. Isolation of *OsHMA9* knockout plants. A, Schematic diagram of *OsHMA9* and insertion positions of T-DNA. Dark-gray boxes represent 10 exons; connecting black lines are nine introns. In line 1B03522, T-DNA was inserted into first intron (*oshma9-1*); in line 3A50792, into the ninth intron (*oshma9-2*) of *OsHMA9*. Horizontal arrows indicate primers (F1, R1, F2, and R2) used for genotyping T2 progeny. Fw, *OsHMA9*-specific forward primer; Rv, *OsHMA9*-specific reverse primer. B, RT-PCR analysis of *OsHMA9* expression. Two replicates for wild type and *oshma9* are shown. *OsHMA9*-specific primers (Fw and Rv) were used for RT-PCR analysis, with total RNA prepared from *oshma9-1*, *oshma9-2*, or wild-type (WT) plants at seedling stage. Rice *actin1* (*OsAct1*) mRNA was amplified to show an equal amount of RNA in each sample.

content were measured to monitor sensitivity to heavy metals (Fig. 8; Supplemental Figs. S5–S8). When both genotypes were reared under normal conditions, all three growth parameters were similar between *oshma9* and wild-type plants (Figs. 7A and 8). However, as concentrations of those four heavy metals increased, performance was inhibited in a dose-dependent manner (Supplemental Figs. S5–S8). Treatment with Cu at less than 100 μM did not lead to significant differences between genotypes, but, at 300 μM Cu, development by the knockout plants was diminished compared with the wild type (Fig. 7; Supplemental Fig. S5). Under such treatment, plant height for *oshma9-1* and *oshma9-2* was reduced to 70% and 81%, fresh weight to 73% and 71%, and chlorophyll content to 75% and 64%, respectively, compared with the wild type (Fig. 8; Supplemental Fig. S5). Likewise, growth of the mutants was retarded in Zn- or Pb-containing medium (Figs. 7 and 8; Supplemental Figs. S6 and S7). These results demonstrate that OsHMA9 is required for conferring tolerance to high levels of Cu, Zn, and Pb. The mutants also showed some sensitivity to Cd, but not as significant as the other metals (Supplemental Fig. S8).

oshma9 Mutants Accumulate More Zn, Cu, Pb, and Cd

If OsHMA9 is indeed a metal efflux transporter, than metal content should be higher in the knockout plants than in wild types. We therefore measured those levels in 12-d-old knockout and wild-type seedlings that had been exposed to high concentrations of heavy metals. When plants were treated with 100 μM Cu, which did not cause any significant growth defects, metal content in shoots did not differ between the mutant and the wild type. However, when grown on medium containing 300 μM Cu, shoots of *oshma9-1*

and *oshma9-2* plants contained 1.3-fold more Cu (Fig. 9). Similarly, higher amounts of Zn, Pb, and Cd were accumulated in the shoots when seedlings were grown with elevated concentrations of those metals. In contrast, none, except Pb, was accumulated in the roots (Fig. 9). Therefore, these results support our conclusion that OsHMA9 is a metal efflux transporter, especially in the shoots.

DISCUSSION

All living organisms must maintain an adequate supply of the metal ions required for vital cellular processes, but it is crucial that these be prevented from accumulating to toxic levels. Tolerance in plants grown on metal-polluted soil can be accomplished either by excluding the uptake mechanisms from the roots, or by metal efflux, compartmentation, and detoxification following that uptake. Interest is growing in research on the metal-transport mechanism to understand the behavior of heavy metals in the soil-plant system. In dicot species, P_{1B}-type ATPases play a role in metal detoxification via efflux (Lee et al., 2003; Williams and Mills, 2005; Andres-Colas et al., 2006). Despite their importance, however, very little is known about the functioning of P_{1B}-type ATPases in monocot species.

In this study, we determined the expression patterns for six members of the Cu cluster. Among them, *OsHMA4*, *OsHMA5*, and *OHMA9* were more preferentially expressed in the roots, whereas the rest were detected almost equally throughout the seedlings. OsHMA9 and OsHMA5 are closely related to Arabidopsis AtHMA7 and AtHMA5, respectively. Expression of *OsHMA4*, *OsHMA7*, and *OsHMA8* was not significantly enhanced under high concentration of Cu, Zn, Pb, or Cd. In contrast, expression of *OsHMA5*, *OsHMA6*, and *OsHMA9* was induced by such treatment, suggesting that at least three OsHMAs (OsHMA5, OsHMA6, and OsHMA9) play roles in heavy-metal detoxification. Among those three, we selected *OsHMA9* for further analysis because it was more specifically induced by Cu and Zn. The *OsHMA9* gene was mainly expressed in vascular tissues, including the xylem and phloem, an observation consistent with a role in the loading and unloading of heavy metals in those tissues. In the leaves, OsHMA9 was also weakly expressed in the mesophyll tissues, a major storage site for heavy-metal ions, again indicating internal detoxification (Ma et al., 2004).

In developing spikelets, expression was strong in the anthers. At the early stages, *OsHMA9* was expressed in all cell types within the anthers. However, in later development, its expression was prominent in the walls. The importance of metal transport in anthers has been previously reported. For example, promoter-GUS fusion analysis of *AtHMA2* and *AtHMA4* has revealed their strong expression in anthers, indicating these two transporters play a specific role in the delivery of Zn to male reproductive tissues (Hussain

Figure 7. Phenotype comparison of wild-type and *oshma9* plants grown under elevated levels of heavy-metal ions. Wild-type, *oshma9-1* (A–E), and *oshma9-2* (F–J) plants were grown for 12 d on solid agar containing one-half-strength Murashige and Skoog medium (A and F), medium supplemented with 5 mM ZnCl$_2$ (B and G), 3 mM lead tartrate (C and H), 500 μM CdCl$_2$ (D and I), or 300 μM CuCl$_2$ (E and J). For each, two plants at left are wild-type control and two plants at right are *oshma9* grown under the same conditions. Bars = 5 cm.
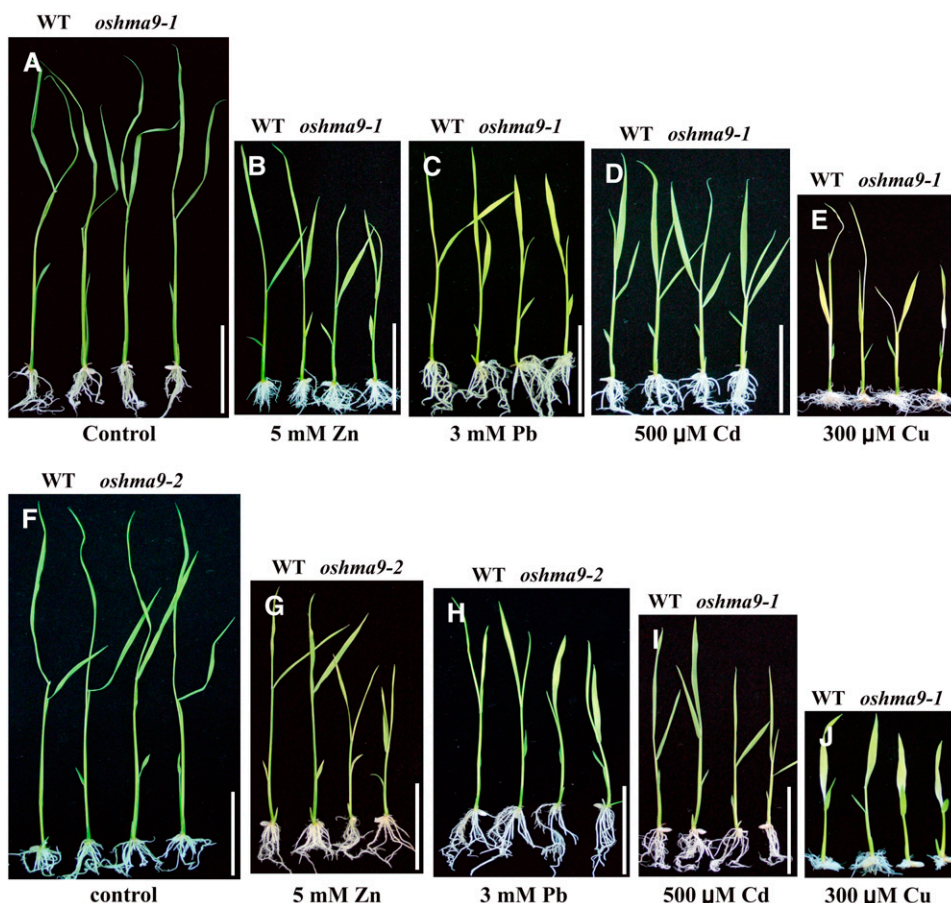
et al., 2004). COPT1, the Arabidopsis high-affinity Cu transporter, also is highly expressed in pollen; defective pollen development in *COPT1* antisense plants is specifically reversed by Cu (Sancenon et al., 2004), supporting a role for its delivery during normal development. *AtHMA5* is as strongly expressed as *COPT1* in the pollen (Andres-Colas et al., 2006). As has been proposed with Arabidopsis, OsHMA9 probably plays a role in metal delivery to rice anthers. Weak expression in the ovary indicates that the protein might also deliver metals in the female organ. However, in our *OsHMA9* knockout plants, we were unable to find any developmental defects in either anther or ovary. Therefore, we might infer that other Cu transporters adequately transport the Cu needed during the formation of those reproductive organs.

To elucidate the functional roles of *OsHMA9* in planta, we assessed the growth of *OsHMA9* knockout plants on medium containing elevated levels of Cu, Zn, Pb, and Cd. For these metals, growth was inhibited compared with the wild type, as manifested by their reduced height, fresh weight, and chlorophyll content. Moreover, the *oshma9* mutant accumulated more Cu, Zn, Pb, and Cd than did the wild type in the shoots. These results indicate that OsHMA9 plays a role in metal detoxification when plants are placed in unfavorable environments, such as with elevated metal ion concentrations. Other evidence for OsHAM9 functioning as an efflux pump arose from our experiments with *E. coli*. Heterologous expression partially rescued the sensitivity to high Cu by the *copA* mutant, which is defective in its endogenous Cu efflux pump. However, *OsHMA9* did not complement the *zntA E. coli* mutant, although disruption of *OsHMA9* led to greater accumulation of Zn in the plants, indicating Zn transport activity. *AtHMA4* confers Cd resistance when expressed in wild-type yeast, but not in the *zntA E. coli* mutant (Mills et al., 2003, 2005). Disruption of *AtHMA4* also results in increased sensitivity to elevated levels of Cd and Zn. These suggest that AtHMA4 serves an important role in metal detoxification at higher metal concentrations (Mills et al., 2005). A range of yeast mutants could be tested to further examine the role of OsHMA9 in Zn transport.

Although the *OsHMA9* gene is expressed in the roots and shows similar metal regulation to the shoots, *oshma9* mutants accumulated metals (apart from Pb) only in the shoots. It is possible that heavy metals are more efficiently sequestered in roots.

OsHMA9 is in the same subclass phylogenetically with AtHMA7/RAN1, which functions in the delivery of Cu ions to the ethylene receptor (Hirayama et al., 1999). Further works are needed to elucidate the roles of OsHMA9 in ethylene-signaling pathways.
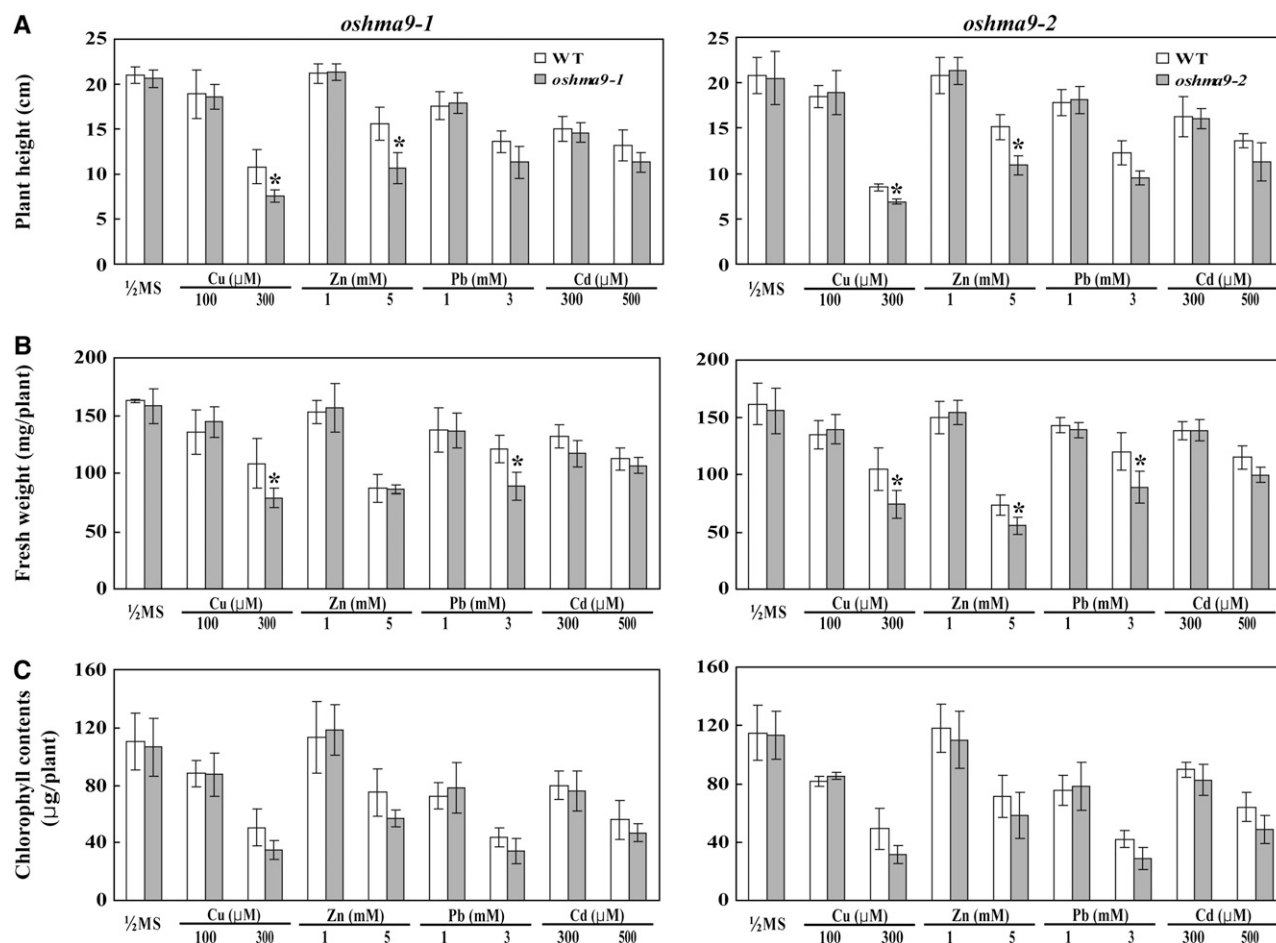
Figure 8. Phenotypic analysis of wild-type and *oshma9* plants grown in medium containing indicated levels of heavy-metal ions. Seeds were germinated and grown for 12 d on one-half-strength Murashige and Skoog agar medium with or without the indicated concentration of $CuCl_2$, $ZnCl_2$, lead tartrate, or 500 μM $CdCl_2$. Height (A) and fresh weight (B) were measured; data are from two independent experiments. In each experiment, eight plants were used for measuring height and fresh weight. Chlorophyll content (C) is average of four plants. Error bars represent SE of 16 replicates for the height and fresh weight and eight replicates for chlorophyll content. Significant differences from wild type were determined by Student's *t* test. *, $P < 0.05$.

Rice contains nine P_{1B}-type HMAs, a number high in comparison with other nonplant eukaryotic species, which have only one or two members (Baxter et al., 2003). None of these rice P_{1B} ATPases has previously been characterized. Arabidopsis has eight members, which have been characterized to some extent (Williams and Mills, 2005; Andres-Colas et al., 2006). Among the rice transporters, OsHMA6 and OsHMA9 form a subclass with Arabidopsis AtHMA7/RAN1, which functions in the delivery of Cu ions (Hirayama et al., 1999). Although *OsHMA6* and *OsHMA9* shared high sequence similarity, their expression patterns differed, with the latter being strongly expressed in roots and the former being expressed mainly in the leaves. *OsHMA9* was more strongly induced by Cu treatment than was *OsHMA6*. These results suggest a divergent role in Cu homeostasis, although both genes require more detailed analyses.

OsHMA9 contains conserved domains present in ATP-driven efflux pump proteins. These include an aspartyl kinase domain (DKTGT), a GDGXNDXP domain (GDGINDSP in OsHMA9), and an E1-E2 ATPase domain characterized by a region with PXD and TGE motifs. The most commonly discussed motif is the heavy-metal-associated domain (Jordan et al., 2001), which typically includes a GMXCXXC sequence. This is present in OsHMA9 in two copies—GMTCSAC and GMTCANC. Research on AtHMA5 has revealed two HMA domains present in the amino-terminal region, both of which interact with Arabidopsis ATX1-like chaperones in vivo, indicating a role for AtHMA5 in metal compartmentalization and detoxification (Andres-Colas et al., 2006). Further work is needed to determine the functional roles of these motifs. Nevertheless, taken together, our results strongly indicate that OsHMA9 is a heavy-metal efflux protein present in the plasma membrane.

Figure 9. Accumulations of Cu, Zn, Pb, and Cd in *oshma9* plants in shoots and roots. Seeds were germinated and grown on for 12 d in one-half-strength Murashige and Skoog solid medium with the indicated concentration of CuCl$_2$, ZnCl$_2$, lead tartrate, or 500 μM CdCl$_2$. Heavy-metal content was measured using atomic absorption spectroscopy. Average of two independent experiments is shown. Significant differences from wild type were determined by Student's *t* test. *, $P <$ 0.05. Bars = SE.
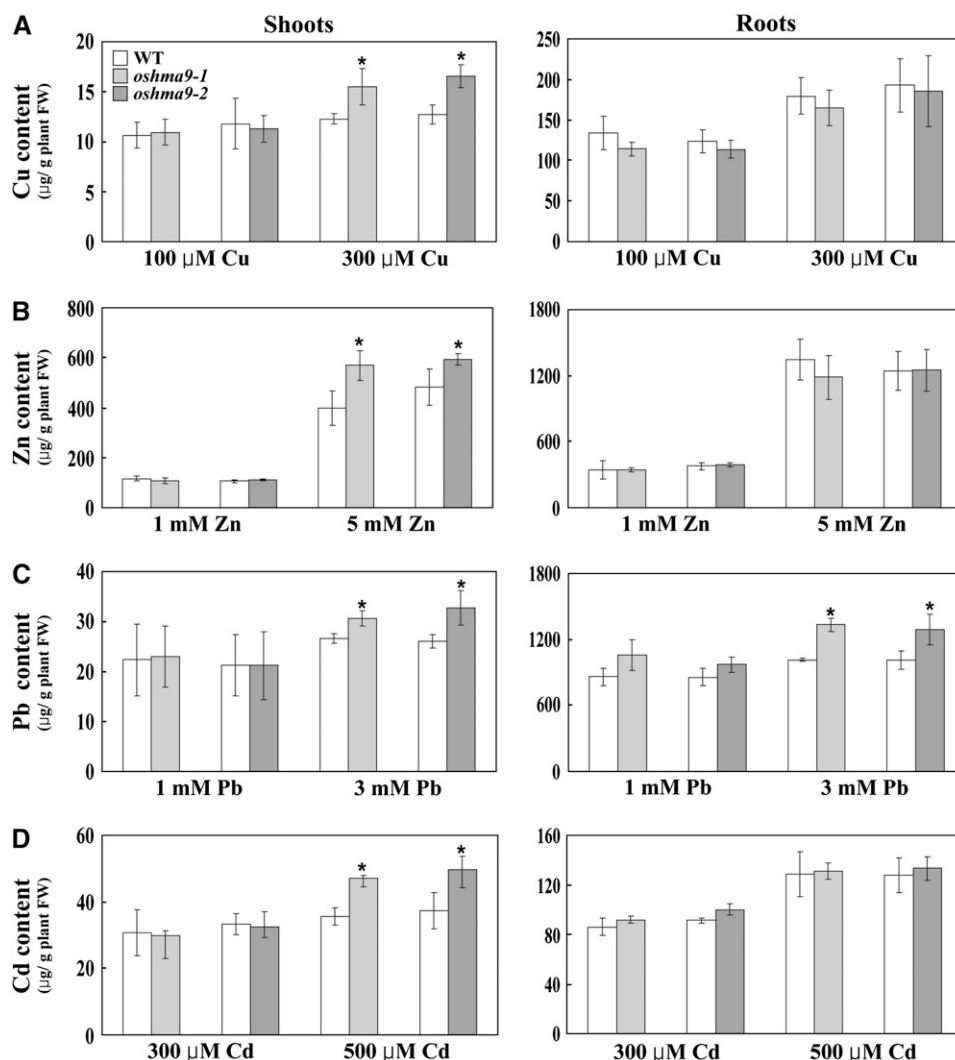
MATERIALS AND METHODS

Plant Growth

Surface-sterilized seeds of *oshma9-1*, *oshma9-2*, and wild-type rice (*Oryza sativa* 'Dongjin') were germinated on one-half-strength Murashige and Skoog medium comprising 1.5% Suc, 0.2% phytagel, and 0.28 mM myoinositol (Sigma). Seedlings were grown for 7 d at 27°C under continuous light, then transferred to soil in the greenhouse and raised to maturity.

Semiquantitative RT-PCR Analysis

Total RNA was isolated from each tissue type with the RNA isolation kit (Tri Reagent; MRC). For cDNA synthesis, we used 2 μg of total RNA as template plus Moloney murine leukemia virus reverse transcriptase (Promega) in a 25-μL reaction mixture. RT-PCR was performed in a 50-μL solution containing a 1-μL aliquot of the cDNA reaction, 0.2 μM of gene-specific primers, 10 mM dNTPs, and 1 unit of rTaq DNA polymerase (TaKaRa Shuzo). PCR conditions included 23 cycles (*OsAct1*) or 25 cycles (*OsHMA4–OsHMA9*) of denaturation at 94°C for 45 s, annealing at 55°C for 45 s, and extension at 72°C for 90 s. We performed a minimal number of cycles to ensure that the reaction was not saturated. PCR products were barely visible when the agarose gels were stained by ethidium bromide. These were separated by electrophoresis on a 1.2% agarose gel, blotted onto a nylon membrane, and hybridized with the ^{32}P-labeled probe specific to each gene, generated from the nonconserved 3' end regions. Primers are shown in Table I. To test the expression levels of

OsHMA4 through *OsHMA9* under heavy-metal stress, 7-d-old plants were floated on one-half-strength Murashige and Skoog medium with or without different concentrations of Cu, Zn, Pb, or Cd. After 3 and 6 h of treatment, leaf and root tissue samples were frozen in liquid nitrogen.

Isolation of *OsHMA9* Knockout Plants

Two *OsHMA9* knockout alleles were isolated from the rice-flanking sequence tag database (http://www.postech.ac.kr/life/pfg). T2 progeny of the primary insertional mutants were grown to maturity to amplify the seeds. Genotypes of the progeny were determined by PCR, with three primers. For the *oshma9-1* line, two *OsHMA9*-specific primers (F1, 5'-TGCAATTTTGG-GTTTTAGCTG-3' and R1, 5'-CTGGGATAATTTCTGCGTCAA-3') and a T-DNA-specific primer (LB-2, 5'-ACGTCCGCAATGTGTTATTAA-3') were used. For *oshma9-2*, the *OsHMA9*-specific primers (F2, 5'-ATCGGCCTTCC-TTTTCTCAT-3' and R2, 5'-TTTCTTTGGCAAGCTCCCTA-3') and a T-DNA-specific primer (RB-2, 5'-CAAGTTAGTCATGTAATTAGCCAC-3') were used.

Construction of the *OsHMA9* Promoter-*GUS* Fusion Molecule and GUS Assay

Genomic sequences (-900 to -1 bp from the translation initiation codon) containing the promoter region of *OsHMA9* were amplified by PCR, using two primers (pf, 5'-AAAAGCTTCACTGTCAGAGCGAAACAAAAATG-3' and pr, 5'-AAAGGATCCGCCGAGAGCTGCAGGTGGGCCAT-3'). The fragment

Table I. *Nucleotide sequences of the primers used for RT-PCR analysis*

Gene	Forward Primer (5′-3′)	Reverse Primer (5′-3′)
OsAct1	GTATCCATGAGACTACATACAACT	TACTCAGCCTTGGCAATCCACA
OsHMA4	CCAACCTTCGAGACTCTTCA	GCATGGGACCTCAGTAAATG
OsHMA5	GGGGCTAATCATGGGGTACT	GAACTCCTGTCTTCGCGTTC
OsHMA6	ATAATGGAGGAGGCCGAACT	CCTGCCTTTTCATGTGGAGT
OsHMA7	TGCTGGGGAAATATCTGGAG	CTTCTGAACTGGAGCCCCTTG
OsHMA8	CGGTGAATGAGAATGGTGTG	TCTTGTCGAAAACGATGCAG
OsHMA9	CAGTAATCGGAGGGACAATG	GTGATGAAACGGTGAAGAGG

was connected to the *GUS-NOSt* cassette (derived from pBI 101.2) and ligated into pCAMBIA1302, resulting in pGA2880. This plasmid was transferred to *Agrobacterium tumefaciens* strain LBA4404 with the freeze-thaw method (An et al., 1988). Transgenic plants carrying the above construct were generated by *Agrobacterium*-mediated cocultivation (Lee et al., 1999). Histochemical GUS staining of transgenic plants was performed according to the method described by Jefferson et al. (1987), except for the addition of 20% methanol to the staining solution (Dai et al., 1996). Sections (10 μm) were prepared as previously described by Jung et al. (2005) and were observed with a microscope (Nikon) under bright- and dark-field illumination.

Subcellular Localization of the OsHMA9-GFP Fusion Protein in Onion Epidermal Cells

Full-length *OsHMA9* cDNA was PCR amplified using the primer pair of gf (5′-AATCTAGACAGGCATGGCCCACCTGCAGCTC-3′) and gr (5′-AAA-GATCTCTACAGTTATCTGCAACACGGTGG-3′). These primers contained *Xba*I or *Bgl*II sites (underlined sequences) to facilitate cloning of the amplified cDNA. After sequence analysis, the *OsHMA9* cDNA was cloned into the *Xba*I and *Bam*HI sites of the 326GFP vector (Lee et al., 2001). The AtAHA2:RFP fusion molecule, under the control of the cauliflower mosaic virus 35S promoter, was obtained from Inhwan Hwang (Pohang University of Science and Technology). Onion (*Allium cepa*) cells were put in Murashige and Skoog medium containing 0.4 mM mannitol during bombardment. The constructs were introduced into onion epidermal cells by particle bombardment with the Biolistic PDS-1000/He Particle Delivery system (Bio-Rad). Expression of GFP and RFP was monitored at 12 h after transformation using a fluorescent microscope (Axioplan2; Carl Zeiss).

Heterologous Expression of *OsHMA9* in *Escherichia coli*

The cDNA fragment containing an entire open reading frame for *OsHMA9* was amplified through RT-PCR with the primer pair F (5′-AAGGTACCCAC-CAAATATTCCCACCTCGCG-3′) and R (5′-AATCTAGAGTGATGAAACG-GTGAAGAGG-3′). These primers contained a *Kpn*I or *Xba*I site (underlined sequences) to facilitate cloning of the amplified cDNA. The fragment was first cloned into the pGEM-T vector (Promega). After sequence analysis, the *OsHMA9* cDNA was subcloned into the *Kpn*I and *Xba*I sites of pBluescript II SK− (Stratagene). The resulting plasmid was introduced into two *E. coli* strains: LMG194 or LMG194 with a *copA* mutation (Rensing et al., 2000). After these strains were grown for 12 h in Luria-Bertani liquid medium containing 0 to 5 mM CuSO$_4$, their cell densities were spectrometrically measured at 600 nm.

Measurements of Plant Growth and Heavy-Metal Content

Wild-type and homozygote *oshma9* seeds were germinated and their seedlings grown for 12 d on solid medium containing one-half-strength Murashige and Skoog salts and supplemented with or without different concentrations of Cu, Zn, Pb, and Cd. Plants were collected and their weights and shoot lengths were measured. To assess their chlorophyll content, leaves were harvested and chlorophyll was extracted with 1 mL 80% acetone from 0.1-g samples. An aliquot of the extracts was taken to measure A_{645} and A_{663} with a spectrophotometer. Specific chlorophyll content was determined according to the method of Arnon (1949). Heavy-metal content was measured as previously described by Kim et al. (2002). Shoots of the 12-d-old plants were harvested and dissolved in 11 N HNO$_3$ in a 200°C oven. Total metal content was then analyzed by atomic absorption spectroscopy (Solaar 989; Unicam Atomic Absorption).

Sequence data from this article can be found in the GenBank/EMBL data libraries under accession number NP_001058305.

Supplemental Data

The following materials are available in the online version of this article.

Supplemental Figure S1. *OsHMA9* promoter-driven GUS expression pattern.

Supplemental Figure S2. Spatial expression pattern of *OsHMA9* in wild-type spikelets.

Supplemental Figure S3. Heterologous expression of *OsHMA9* in *E. coli*.

Supplemental Figure S4. RT-PCR analysis of the *OsHMA9* transcript in *oshma9* and wild-type plants.

Supplemental Figure S5. Height, fresh weight, and chlorophyll content of plants grown on medium containing different concentrations of Cu.

Supplemental Figure S6. Height, fresh weight, and chlorophyll content of plants grown on medium containing different concentrations of Zn.

Supplemental Figure S7. Height, fresh weight, and chlorophyll content of plants grown on medium containing different concentrations of Pb.

Supplemental Figure S8. Height, fresh weight, and chlorophyll content of plants grown on medium containing different concentrations of Cd.

LITERATURE CITED

Abdel-Ghany SE, Muller-Moule P, Niyogi KK, Pilon M, Shikanai T (2005) Two P-type ATPases are required for copper delivery in *Arabidopsis thaliana* chloroplasts. Plant Cell **17:** 1233–1251

An G, Ebert PR, Mitra A, Ha SB (1988) Binary vectors. *In* SB Gelvin, RA Schilperoort, eds, Plant Molecular Biology Manual. Kluwer Academic Publishers, Dordrecht, The Netherlands, pp 1–19

An S, Park S, Jeong DH, Lee DY, Kang HG, Yu JH, Hur J, Kim SR, Kim YH, Lee M, et al (2003) Generation and analysis of end sequence database for T-DNA tagging lines in rice. Plant Physiol **133:** 2040–2047

Andres-Colas N, Sancenon V, Rodriguez-Navarro S, Mayo S, Thiele DJ, Ecker JR, Puig S, Penarrubia L (2006) The Arabidopsis heavy metal

P-type ATPase HMA5 interacts with metallochaperones and functions in copper detoxification of roots. Plant J **45:** 225–236

Arnon DI (1949) Copper enzymes in isolated chloroplasts: polyphenoloxidase in *Beta vulgaris.* Plant Physiol **24:** 1–15

Axelsen KB, Palmgren MG (1998) Evolution of substrate specificities in the P-type ATPase superfamily. J Mol Evol **46:** 84–101

Axelsen KB, Palmgren MG (2001) Inventory of the superfamily of P-type ion pumps in Arabidopsis. Plant Physiol **126:** 696–706

Baxter I, Tchieu J, Sussman MR, Boutry M, Palmgren MG, Gribskov M, Harper JF, Axelsen KB (2003) Genomic comparison of P-type ATPase ion pumps in Arabidopsis and rice. Plant Physiol **132:** 618–628

Broadley MR, White PJ, Hammond JP, Zelko I, Lux A (2007) Zinc in plants. New Phytol **173:** 677–702

Clemens S (2001) Molecular mechanisms of plant metal tolerance and homeostasis. Planta **212:** 475–486

Colangelo EP, Guerinot ML (2006) Put the metal to the petal: metal uptake and transport throughout plants. Curr Opin Plant Biol **9:** 322–330

Dai Z, Gao J, An K, Lee JM, Edwards GE, An G (1996) Promoter elements controlling developmental and environmental regulation of a tobacco ribosomal protein L34. Plant Mol Biol **32:** 1055–1065

Eren E, Arguello JM (2004) Arabidopsis HMA2, a divalent heavy metal-transporting P(IB)-type ATPase, is involved in cytoplasmic Zn^{2+} homeostasis. Plant Physiol **136:** 3712–3723

Fernandes JC, Henriques FS (1991) Biochemical, physiological, and structural effects of excess copper in plants. Bot Rev **57:** 246–273

Goff SA, Ricke D, Lan TH, et al (2002) A draft sequence of the rice genome (*Oryza sativa* L. ssp. *japonica*). Science **296:** 92–100

Gravot A, Lieutaud A, Verret F, Auroy P, Vavasseur A, Richaud P (2004) AtHMA3, a plant P1B-ATPase, functions as a Cd/Pb transporter in yeast. FEBS Lett **561:** 22–28

Grotz N, Guerinot ML (2006) Molecular aspects of Cu, Fe and Zn homeostasis in plants. Biochim Biophys Acta **1763:** 595–608

Himelblau E, Amasino RM (2001) Nutrients mobilized from leaves of Arabidopsis thaliana during leaf senescence. J Plant Physiol **158:** 1317–1323

Hirayama T, Kieber JJ, Hirayama N, Kogan M, Guzman P, Nourizadeh S, Alonso JM, Dailey WP, Dancis A, Ecker JR (1999) RESPONSIVE-TO-ANTAGONIST1, a Menkes/Wilson disease-related copper transport, is required for ethylene signaling in Arabidopsis. Cell **97:** 383–393

Hussain D, Haydon MJ, Wang Y, Wong E, Sherson SM, Young J, Camakaris J, Harper JF, Cobbett CS (2004) P-type ATPase heavy metal transporters with roles in essential zinc homeostasis in *Arabidopsis.* Plant Cell **16:** 1327–1339

International Rice Genome Sequencing Project (2005) The map-based sequence of the rice genome. Nature **11:** 793–800

Jefferson RA, Kavanagh TA, Bevan MW (1987) GUS fusions: beta-glucuronidase as a sensitive and versatile gene fusion marker in higher plants. EMBO J **6:** 3901–3907

Jeon JS, Lee S, Jung KH, Jun SH, et al (2000) T-DNA insertional mutagenesis for functional genomics in rice. Plant J **22:** 561–570

Jeong DH, An S, Kang HG, Moon S, Han JJ, Park S, Lee HS, An K, An G (2002) T-DNA insertional mutagenesis for activation tagging in rice. Plant Physiol **130:** 1636–1644

Jeong DH, An S, Park S, Kang HG, Park GG, Kim SR, Sim J, Kim YO, Kim MK, Kim SR, et al (2006) Generation of a flanking sequence-tag database for activation-tagging lines in japonica rice. Plant J **45:** 123–132

Jordan IK, Natale DA, Koonin EV, Galperin MY (2001) Independent evolution of heavy metal-associated domains in the copper chaperones and copper-transporting ATPases. J Mol Evol **53:** 622–633

Jung KH, Han MJ, Lee YS, Kim YW, Hwang I, Kim MJ, Kim YK, Nahm BH, An G (2005) Rice Undeveloped Tapetum1 is a major regulator of early tapetum development. Plant Cell **17:** 2705–2722

Kim DH, Eu YJ, Yoo CM, Kim YW, Pih KT, Jin JB, Kim SJ, Stenmark H, Hwang I (2001) Trafficking of phosphatidylinositol 3-phosphate from the trans-golgi network to the lumen of the central vacuole in plant cells. Plant Cell **13:** 287–301

Kim YY, Yang YY, Lee Y (2002) Pb and Cd uptake in rice roots. Physiol Plant **116:** 368–372

Krämer U, Talke IN, Hanikenne M (2007) Transition metal transport. FEBS Lett **581:** 2263–2272

Kuhlbrandt W (2004) Biology, structure and mechanism of P-type ATPases. Nat Rev Mol Cell Biol **5:** 282–295

Lee J, Bae H, Jeong J, Lee JY, Yang YY, Hwang I, Martinoia E, Lee Y (2003) Functional expression of a bacterial heavy metal transporter in Arabidopsis enhances resistance to and decreases uptake of heavy metals. Plant Physiol **133:** 589–596

Lee S, Jeon JS, Jung KH, An G (1999) Binary vector for efficient transformation of rice. J Plant Biol **42:** 310–316

Lee YJ, Kim DH, Kim YW, Hwang I (2001) Identification of a signal that distinguishes between the chloroplast outer envelope membrane and the endomembrane system in vivo. Plant Cell **13:** 2175–2190

Ma JF, Ueno D, Zhao FJ, McGrath SP (2004) Subcellular localisation of Cd and Zn in the leaves of a Cd-hyperaccumulating ecotype of Thlaspi caerulescens. Planta **220:** 731–736

Mills RF, Francini A, Ferreira da Rocha PS, Baccarini PJ, Aylett M, Krijger GC, Williams LE (2005) The plant P_{1B}-type ATPase AtHMA4 transports Zn and Cd and plays a role in detoxification of transition metals supplied at elevated levels. FEBS Lett **579:** 783–791

Mills RF, Krijger GC, Baccarini PJ, Hall JL, Williams LE (2003) Functional expression of AtHMA4, a P1B-type ATPase of the Zn/Co/Cd/Pb subclass. Plant J **35:** 164–176

Pedersen P, Carafoli E (1987) Ion motive ATPases. I. Ubiquity, properties, and significance to cell function. Trends Biochem Sci **4:** 146–150

Rensing C, Fan B, Sharma R, Mitra B, Rosen BP (2000) CopA: an *Escherichia coli* Cu(II)-translocating P-type ATPase. Proc Natl Acad Sci USA **97:** 652–656

Rensing C, Ghosh M, Rosen BP (1999) Families of soft-metal-ion-transporting ATPases. J Bacteriol **181:** 5891–5897

Rensing C, Mitra B, Rosen BP (1997) The zntA gene of *Escherichia coli* encodes a Zn(II)-translocating P-type ATPase. Proc Natl Acad Sci USA **94:** 14326–14331

Rout GR, Das P (2003) Effect of metal toxicity on plant growth and metabolism: I. Zinc. Agronomie **23:** 3–11

Ryu CH, You JH, Kang HG, Hur J, Kim YH, Han MJ, An K, Chung BC, Lee CH, An G (2004) Generation of T-DNA tagging lines with a bidirectional gene trap vector and the establishment of an insertion-site database. Plant Mol Biol **54:** 489–502

Sancenon V, Puig S, Mateu-Andres I, Dorcey E, Thiele DJ, Penarrubia L (2004) The Arabidopsis copper transporter COPT1 functions in root elongation and pollen development. J Biol Chem **279:** 15348–15355

Schutzendubel A, Polle A (2002) Plant responses to abiotic stresses: heavy metal-induced oxidative stress and protection by mycorrhization. J Exp Bot **53:** 1351–1365

Seigneurin-Berny D, Gravot A, Auroy P, Mazard C, Kraut A, Finazzi G, Grunwald D, Rappaport F, Vavasseur A, Joyard J, et al (2006) HMA1, a new Cu-ATPase of the chloroplast envelope, is essential for growth under adverse light conditions. J Biol Chem **281:** 2882–2892

Shikanai T, Muller-Moule P, Munekage Y, Niyogi KK, Pilon M (2003) PAA1, a P-type ATPase of *Arabidopsis*, functions in copper transport in chloroplasts. Plant Cell **15:** 1333–1346

Tabata K, Kashiwagi S, Mori H, Ueguchi C, Mizuno T (1997) Cloning of a cDNA encoding a putative metal-transporting P-type ATPase from *Arabidopsis thaliana*. Biochim Biophys Acta **1326:** 1–6

Verret F, Gravot A, Auroy P, Leonhardt N, David P, Nussaume L, Vavasseur A, Richaud P (2004) Overexpression of AtHMA4 enhances root-to-shoot translocation of zinc and cadmium and plant metal tolerance. FEBS Lett **576:** 306–312

Williams LE, Mills RF (2005) P_{1B}-ATPases—an ancient family of transition metal pumps with diverse functions in plants. Trends Plant Sci **10:** 491–502

Williams LE, Pittman JK, Hall JL (2000) Emerging mechanisms for heavy metal transport in plants. Biochim Biophys Acta **1465:** 104–126

Yu J, Hu S, Wang J, et al (2002) A draft sequence of the rice genome (*Oryza sativa* L. ssp. *indica*). Science **296:** 79–92